Assessment of Pb-induced stress levels on rice based on fractal characteristic of spectral high-frequency components

LIU Meiling, LIU Xiangnan, CAO Shi, LI Ting, WU Ling

School of Information Engineering, *China University of Geosciences*, *Beijing* 100083, *China*

Abstract: How to extract and calculate subtle spectral feature information of crop under various environmental-induced stresses from hyperspectral remote sensing is crucial for the application of remote sensing in monitoring agricultural pollution. The objective of this paper is to monitor the stress levels of rice under the Pb pollution. Hyperspectral data and heavy metal content were collected in the field experiment. The fifth level high—frequency component (d5) was obtained by performing wavelet transform to hyperspectral reflectance (350-1300 nm) and the fractal dimension of d5 was also calculated. Then the relationship between fractal dimension of d5 and different stress levels of rice was established by the fuzzy logic model. The results showed that: (1) d5 can effectively distinguish the stress levels of rice Pb pollutions; (2) the annual relative variation ratio for fractal dimension of d5 was below 4%, and the classification accuracy of fractal dimension of d5 was above 75%. Namely, fractal dimension values of d5 for rice under high, medium and low pollutions have percentage of 86.7% between 1.160 and 1.200, 75% between 1.220 and 1.275, 91.7% between 1.280 and 1.320, respectively. (3) the high (low) semi-trapezoidal functions were carried out to construct a model to detect stress levels of rice.

Key words: hyperspectral reflectance, wavelet transform, fractal analysis, membership function, rice, Pb-induced stress

CLC number: S127 **Document code:** A

Citation format: Liu M L, Liu X N, Cao S, Li T and Wu L. 2011. Assessment of Pb-induced stress levels on rice based on fractal characteristic of spectral high- frequency components. *Journal of Remote Sensing*, **15**(4): 811–830

1 INTRODUCTION

Heavy metal contamination in agricultural soil is one of the important ecological environmental problems, which is characterized by serious toxicity, strong concealment and complicated ecological effects (Wang & Zhang, 2002; Qi, *et al*., 2008). It is reported that the area of soil heavy metal contamination in China is 2×10^7 hm^2, accounting for 1/6 of the total area of farmland (Zhao, *et al*., 2002a). In Jiangsu Province, China, the ratio of Pb content in foodstuff (such as rice and wheat) serious than food quality standard is 21.4% and values of specific local regions even have reached as high as 66 % (Zhao, *et al*., 2002b). Due to the rapid economic development of society and environmental protection measure remaining lagging, heavy metal pollution in agricultural soil has become more and more serious. Therefore, accurate and fast detection of heavy metal-induced stress in crops is critical for agricultural ecology and food security. To date, the detection, simulation and assessment of status, dynamic process and change in crops under heavy metal pollution are the important issues for the application the hyperspectral remote sensing in precision agriculture (Kooistra, *et al*., 2001; Osborne, *et al*., 2002; Dunagan, *et al*., 2007; Montzka, *et al*., 2008). The emergence of hyperspectral data has led to its widespread and fast use in detecting heavy metal pollution and crop stress due to their capabilities in detecting variations in biochemical compositions. Excessive heavy metal concentrations in plant can affect its biochemical composition (such as chlorophyll content and nutritious component), which can be reflected in hyperspectral reflectance. Therefore, some researches applied hyperspectral reflectance directly to detect the stress of plant under heavy metal pollution. Choe, *et al*. (2008) established relationships between heavy metal content in abandoned mines and reflectance characteristics, biochemical composition, and pigment content of the plants (Choe, *et al*., 2008; Li, *et al*., 2008). Clevers, *et al*. (2004) monitored heavy metal contamination in river floodplains by exploring field vegetation indices and the positions of the red edge (Clevers, *et al*., 2004; Kooistra, *et al*., 2004). They demonstrated that spectral characteristic parameters in some wavebands are regarded as effective indicators for detecting soil heavy metal contaminations. Specifically, these experiments were performed under laboratory conditions to analyze the effect of heavy metal on

Received: 2010-04-22; **Accepted:** 2010-08-20

Foundation: National Natural Science Foundation of China (No.40771155); National High-tech R&D Program of China (863 Program) (No.2007AA12Z174)

First author biography: LIU Meiling (1978—), female, doctor, she received BS and MS degrees from Hunan Normal University and China University of Geosciences(Beijing). Her current research interests include remote sensing applications. E-mail: liumeiling427@126.com

Corresponding author: LIU Xiangnan (1964—), male, doctor, His research interests are remote sensing information analysis and application of geosciences. E-mail: liuxncugb@163.com

spectral reflectance of controlled crop. Collins, *et al*. investigated the variation in spectral reflectance, such as chlorophyll absorption valley and red edge of sorghum, mustard, and fern, under laboratory conditions by adding different doses of copper, lead, zinc, or arsenic (Collins, *et al*., 1983; Schuerger, *et al*., 2003; Slonecker, *et al*., 2009). Similarlly, Liu, *et al*. also investigated the changes in spectral reflectance of wheat, cabbage, and rice, under laboratory conditions by adding copper, zinc or lead (Liu, *et al*., 2006; Chen, *et al*., 2007; Ren, *et al*., 2008). The above results showed that there were strong relationships between the blue-shift of 'red edge', the changes in near-infrared reflectance and chlorophyll concentration, heavy metal content in crops. Many researches demonstrate that the obvious changes (such as the blue shift of 'red edge', shallow chlorophyll absorption valley, near infrared reflectance plateau lowering) in spectral reflectance of crops occurred are due to changes in physiological parameters of crops under high pollutions. However, the level of pollutants in natural ecosystems is relatively low, which means that there may be no visible and steady symptoms in leaf reflectance spectra. And therefore it is necessary to develop spectral analysis methods to enhance the vegetative stress signals through minimizing the effects of background materials, such as those caused by non-photosynthetic components and soil reflectance. Recently, some studies extract the diagnostic spectral index to detect and assess the stress levels of plant under heavy metal pollution through the approaches of enhancement and transformation of the original spectrum, such as spectral absorption feature parameters, multi-dimensional spectral index space, artificial neural network or fractal technology (van der Meer, 2006; Noh, *et al*., 2006; Wang, *et al*., 2006; Guan & Liu, 2009; Du, *et al*., 2009). However, the spectral feature information associated with heavy metal pollution is subtle, as well as random and uncertain on a large scale. Thus, it is difficult to extract the weak spectral characteristic information of polluted crops only applying some simple or single method for spectral analysis.

The objective of this research is to detect and assess the stress levels of rice under heavy metal pollution based on wavelet transform, fractal techniques in combination with fuzzy mathematics. The results of our study may provide scientific reference for the enhancements, calculation and modeling the subtle spectral characteristic information associated with environmental-induced stress on crop. It can provide some insights into identifying Pb pollution in natural agricultural ecosystems.

2 MATERIALS AND METHODS

2.1 Field experiment design and data collection

Field experiments, which is located in Dongqiao and Zhengyi town in Suzhou, Jiangxu Province, China, were conducted in three different contaminated levels with high, medium and low pollution (labeled as A, B, and C respectively). The crop selected in this site was rice, which belongs to one Changyou species. The rice growing in the three experiment field were cultivated scientifically, and supplied with abundant fertilizers, manures and irrigation water to avoid other environmental factors causing unwanted stress. The site where located has a warm and humid subtropical climate with an annual temperature of 15.7° C, rainfall of 1094 mm and average sunshine of 1965 h. Soils are mainly paddy soils formed on calcareous deposits of the Yangtze River with sufficient organic matter about 3% and soil pH of 6.2. The main heavy metal contents of the soil are presented in Table 1.

The hyperspectral data collections were carried out in clear days in 2008 and 2009 according to critical growth stages of rice, which corresponded to the seedling, tillering, jointing, anthesis and mature growth stages of rice. Spectral measurements were taken under cloudless or near-cloudless conditions between 10:00 and 14:00, using an ASD FieldSpec Pro spectrometer (Analytical Spectral Devices, Boulder, Co., USA). This spectrometer was fitted with a 10° field of view fiber optics, operated in the 350—2500 nm spectral regions with sampling intervals of 2 nm. $BaSO_4$ calibration panel was used for calculating the black and baseline reflectance. A panel radiance measurement was taken before and after the crop measurement by 2 scans each time. Rice radiance measurement was made at 30—40 sites over each plot and each site was scanned 10 times. The biochemistry data of soils and rice was collected to synchronize spectral measurements. Heavy metal concentration (Cu, Zn, Pb, Cd, Cr and As) in the soil were determined by flame atomic absorption spectrometry (AAS).

Table 1 The heavy metal concentrations of agricultural soil in experimental sites

Experimental sites	Geographical location	Background (Ci)	As	Cr	Cu	Zn	Pb	Cd	Pollution level
			13.6	62.6	24.4	80.1	29.1	0.065	
A	31°25′ N, 120°31′ E	Mean (Si)	8.90	54.2	23.8	78.5	128.3	0.097	High
		Polluted index (Pi)	0.65	0.87	0.98	0.98	4.41	1.49	
B	31°24′ N, 120°33′ E	Mean (Si)	7.20	60.5	22.3	59.3	71.7	0.082	Medium
		Polluted index (Pi)	0.53	0.97	0.91	0.74	2.46	1.26	
C	31°21′ N, 120°51′ E	Mean (Si)	6.50	61.4	23.9	37.4	30.8	0.04	Low
		Polluted index (Pi)	0.48	0.98	0.98	0.47	1.05	0.66	

Note: Ci is Background value of heavy metal concentrations according to the Environment Monitoring Centre of China. Si is measured value of heavy metal concentrations, $Pi=Ci/Si$, Pollution level is classified as low ($1<Pi<2$), medium ($2<Pi<3$) or high ($Pi>3$).

2.2 Methods

To effectively detect and amplify subtle spectral characteristic information associated with heavy metal pollution, methods based on wavelet transform, fractal analysis in combination with fuzzy mathematics were used. The procedure can be summarized as the following (Fig.1). Firstly, the wavelet high-frequency component was generated at each level of decomposition of an original spectral signal to derive and enhance subtle spectral characteristic information associated with rice under heavy metal stress. The reason is that wavelet transform has proven to be quite useful in the study of spectral smoothing, noise removal and singularity signal detecting. Secondly, fractal dimension of the fifth high-frequency component was explored as a new comprehensive parameter to quantitatively analyze stress levels of rice under heavy metal pollution. Thirdly, the fuzzy logic model was established between fractal dimension of high-frequency component and stress levels of rice under heavy metal pollution by using the membership function.

2.2.1 *Extracting spectral high-frequency component through wavelet transform*

Wavelets are mathematical functions that are used to dissect data into different frequency components and each component is characterized with a resolution appropriate to its scale. Wavelet transforms (WT) can be viewed as a rotation from function space into a different domain, which contains an infinite set of possible basis functions called mother wavelets. WT has excellent time and frequency properties, and therefore it is suitable to detect signal singularity, which are discontinuous (shocks) points at x0 waveband in original spectrum signals or derivatives of the spectrum signals (Daubechies, 1990). Many wavelet functions have been widely used in solving a range of real world problems. However, the selection of wavelet function depends on different signal processing problems. Previous result showed the Daubechies wavelets ('db5') was able to detect stress information in a satisfactory way by reducing impacts of atmospheric scattering, absorption, background and equipment noise on spectral signal of rice (Liu, *et al*.,2010). In this research, WT was implemented by using a dyadic filter tree. The wavelet low-frequency component (a) and high-frequency component (d) were generated at each level of decomposition (denoted by subscript numbers) of an original signal. An inverse discrete wavelet transform can accurately reconstruct the original signal as all of information in the original signal is contained in the low-frequency component at a particular level plus the high-frequency component at that level plus previous levels by the following equation:

$$f(\lambda) = a_j(\lambda) + \sum_{i=1}^{j} d_i(\lambda) \tag{1}$$

where $f(\lambda)$ is original spectral signal, j is wavelet decomposition level, a_j and d_i are the wavelet low-frequency component and high-frequency component, respectively. Low-frequency signals (signals with relatively stable) can reflect the global characteristic of the signal spectrum, due to it is characterized by high frequency resolution and low band (time) resolution. While high-frequency signals can be used in the analysis of nonstationary signals and have particular advantages for detecting short-lived and singularity phenomena. This is because high-frequency signals have the property of high band resolution and low frequency resolution and thus obtain information on the frequency variations of these signals and to detect their structures localization in time and/or in space. In this research, wavelet disassembled signal were performed by wavelet transform to original hyperespectral reflectance (350—1300 nm) with Daubechie 5 (db5) wavelet function. The result showed that the five decomposition levels were able to detect stress information of rice under heavy metal pollution in a satisfactory way. In five decomposition levels, the behavior of the wavelet component for spectral data at levels *j*= 1, 2, 3, 4, 5, denoted by a5 for low-frequency wavelet component, d1, d2, d3, d4 and d5 for high-frequency wavelet component (Fig. 1). As seen in Fig. 1, large amplitude of d1, d2, d3 and d4 present noise signal and the large amplitude of

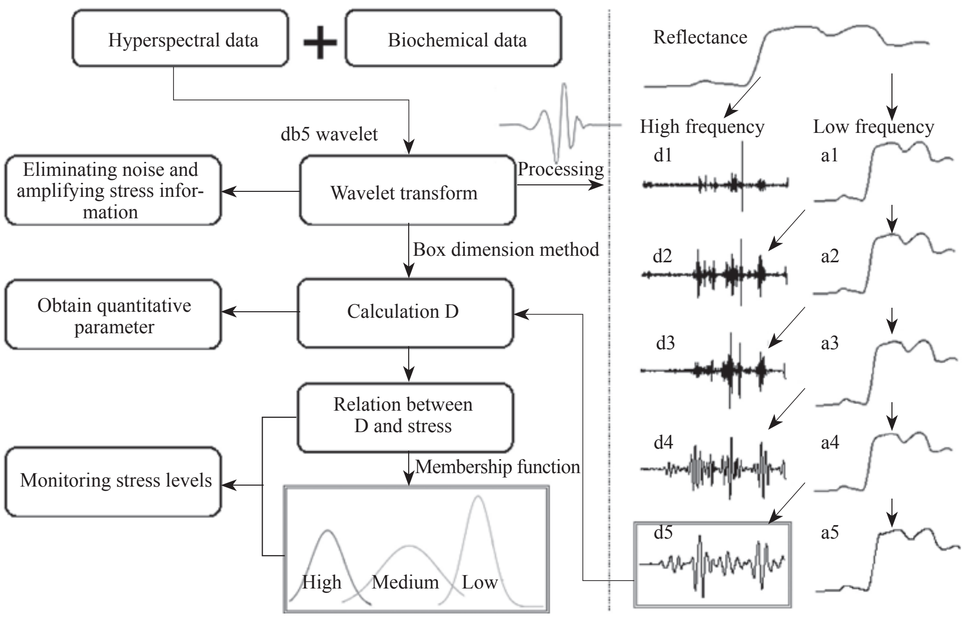

Fig. 1 The general flow chart of deriving, calculating and establishing models for metal-induced spectral subtle information

d5 present singularity signals. It is concluded that five decomposition levels are determined to be the most appropriate level for both identifying the stress levels of rice under heavy metal pollution and removing noise.

2.2.2 *Calculating fractal dimension of high-frequency component*

Fractals, here referring to broken or irregular fragments, can describe complex and irregular natural objects. A number of studies demonstrate that remote sensing images and hyperspectral reflectance are proved to have fractal characteristics (Du, *et al*., 2009). Similarly, d5, which belongs to the fraction of original reflectance, has fractal properties. In order to comprehensively and accurately compare and quantify subtle spectral characteristics information of rice under different Pb pollutions, the fractal dimension of fifth high frequency component (d5) is calculated by the fractal technology. The two reasons are as follows. Firstly, fractal analysis is consistent with wavelet transform in 'scaling transformation' and 'self-similarity' of signal. Secondly, fractal dimensions can be used to explain the comprehensive variations of spectrum curves as a 'global parameter'. Therefore, it has the advantage of capturing more information provided by reflectance spectra than previous analytical approaches and thus improves the sensitivity of spectral parameter for investigating changes in plant stress.

Fractal dimension are commonly calculated by using the methods for box-counting dimension, isarithm dimension and Hausdorff dimension, *etc*. In this study, fractal dimensions are calculated by the box-counting method which is based on the division of an area into regular boxes with the same box edge length value of n (Borodich, 1997). The equation is as follows:

$$D = \lim_{n\to\infty} \frac{\log_2 M(n)}{\log_2 n} \tag{2}$$

where D is the fractal dimension, $M(n)$ and n is the count of boxes in the grid divided curve and scales, respectively.

2.2.3 *Establishing membership function between fractal dimension and stress levels of rice under heavy metal pollution*

It is well-known that fuzzy model serves as an appropriate mathematical tool for solving fuzzy and uncertain problems. The spectral characteristic of rice under heavy metal pollution is very complex, which is predominantly contributed by the complicated response mechanism of spectrum on the variation of physiological and biochemical compositions in rice under heavy metal pollution. Considering that the stress levels assessment is a fuzzy concept with multiple indicators and classes, membership functions of fuzzy set theory are used, which have been proved effective in solving problems of fuzzy boundaries and avoid the effect of subjective factors on assessment results. The typical methods for establishment membership function include high (lower) semi-trapezoidal functions, Gaussian membership function and triangular membership function. In this study, high (lower) semi-trapezoidal functions were selected to construct models between fractal dimension of d5 and stress levels of rice under heavy metal pollution. The stress levels were determined by the function degree of measured fractal dimension values of d5, which belonged to different membership functions according to the domain of fractal dimension of d5.

3 RESULTS

3.1 Response mechanism of fractal characteristic of high-frequency components on stress levels of rice under Pb pollution

In general, the singularity of the spectrum is caused by the discontinuous of signal in some distinctive absorption features. The primary reason is that the phenomena of electron or atoms transition and the shift of inherent absorption characteristic bands or regions (chlorophyll absorption) in crop could be exhibited in reflectance spectra. When rice is stressed by Pb pollution, the change of shift and amplitude in singularity (shocks) points occurs, because heavy metal can lead atoms or ions coming into the rice and further destroying the molecular environment. However, it is difficult to indentify the singularity points in the original spectrum. The extraction of subtle characteristic spectral information associated with heavy metal stress is necessary for monitoring heavy metal pollution, and a reliable method for detecting signal singularity points is wavelet transform. Since wavelet transform has an excellent time and frequency property. It can make the interested component submerged in an original signal become distinct under certain scales. Singularity points of spectral signal across the specific bands can be quantitatively calculated and analyzed (Fig. 2). As seen in Fig. 2, the difference of positions and amplitudes of singularity points in d5 curves of rice with differing heavy metal pollution were displayed. Such differences can serve as a basis for distinguishing the stress levels of rice under heavy metal pollution. Compared with the singularity points of rice under low pollution, the variations of singularity points were calculated, including the shift of singularity position and singularity amplitude of rice under high and medium pollution (Table 2). As shown in Table 2, regardless of the rice under high pollution and medium pollution, the variation of singularity position and singularity amplitude were observed. In detail, there were apparent shifts of singularity position in the spectral region between 696 nm and 788 nm. While obvious shifts of singularity amplitude occurred in the spectra between 876 nm and 1183 nm. In order to explain the overall variation of spectral singularity points of rice under differing Pb pollution, the fractal dimension of d5 for all rice samples was calculated and summarized. The values of fractal dimension of d5 curve in rice under high, medium and low pollution were 1.232, 1.267 and 1.290, respectively, from Fig. 2. Low values in fractal dimension of d5 indicated that the rice was suffering from very serious contamination.

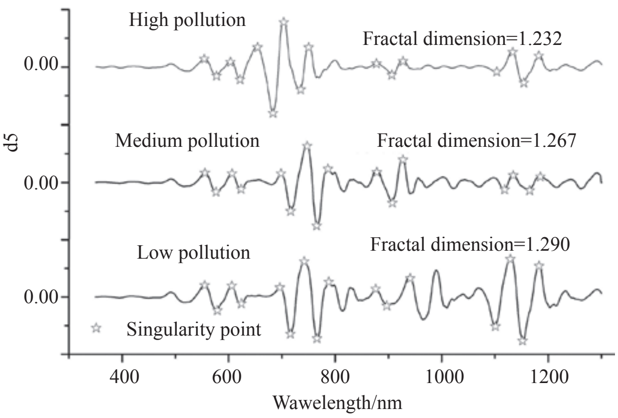

Fig. 2 The singularity points of spectrum in rice under different heavy metal pollutions

Table 2 The shift and amplitude of singularity points for spectrum in rice under different heavy metal pollutions

Pollution level*	Singularity points of rice under low pollution	555	579	606	624	696	716	742	766	788	876	897	941	1101	1129	1152	1183
High-Low	Shift / nm	– 1	– 2	– 3	– 3	– 42	– 33	– 39	– 31	– 38	1	9	– 1	– 2	– 3	– 3	– 42
	Amplitude / %	32	34	56	91	106	25	26	46	31	57	10	69	83	61	64	64
Medium-Low	Shift / nm	0	– 3	0	– 1	2	0	5	– 1	– 2	2	10	– 14	17	5	13	2
	Amplitude / %	20	30	21	0	6	22	2	4	10	29	129	22	76	81	82	81

Note: *The variation is based on high and medium pollution according to low pollution as standard value. Amplitude $=|a-b|/|b|$. Here, b is d5 value corresponding to singularity points of rice under low pollution, a is d5 value corresponding to singularity points of rice under high or medium pollution.

3.2 Analyzing spectral characteristic of high-frequency component of rice at different growth stages

To illustrate spectral characteristic of high-frequency component of rice at different growth stages, hyperspectra data from seedling stage, tillering stage, jointing stage, anthesis and maturity growth stage of rice were obtained for different levels of heavy metal pollution. For clarity, the average value from 200 data sets of each growth stage in different level pollution respectively were calculated and then performed by fifth wavelet decomposition level with 'Db5' wavelet function. Fig. 3 showed the d5 curve of rice at five growth stages for different levels of Pb pollution. As shown in Fig. 3, the obvious variation of d5 curve of rice under high pollution was validated. The number of extreme points is increasingly becoming large. And also the curve is becoming more complex from the seedling stage to maturity. The fractal dimension and singularity amplitude of d5 of rice under different level pollutions at each growth stage were shown in Table 3. From Table 3, regardless of rice under contaminated levels, it can be seen that the singularity amplitude increased from seedling to tillering and then decreased from tillering to mature growth stage. The maximum value in singularity amplitude in rice with different pollution levels occurred at the tillering growth stage. The reason is that the maximum velocity of heavy metal diffusion in rice occurred at the tillering growth stage. Therefore, in this study, the tillering growth stage was selected as best growth stage for detecting heavy metal concentrations in rice to distinguish different heavy metal stress levels. Whereas, fractal dimension of d5 increased from seedling, tillering, jointing, anthesis to mature in the whole growth stage. This can be interpreted by the shock points that are increasingly becoming large and then spectral curve is becoming more complex with the increase of Pb diffusion in rice from soil.

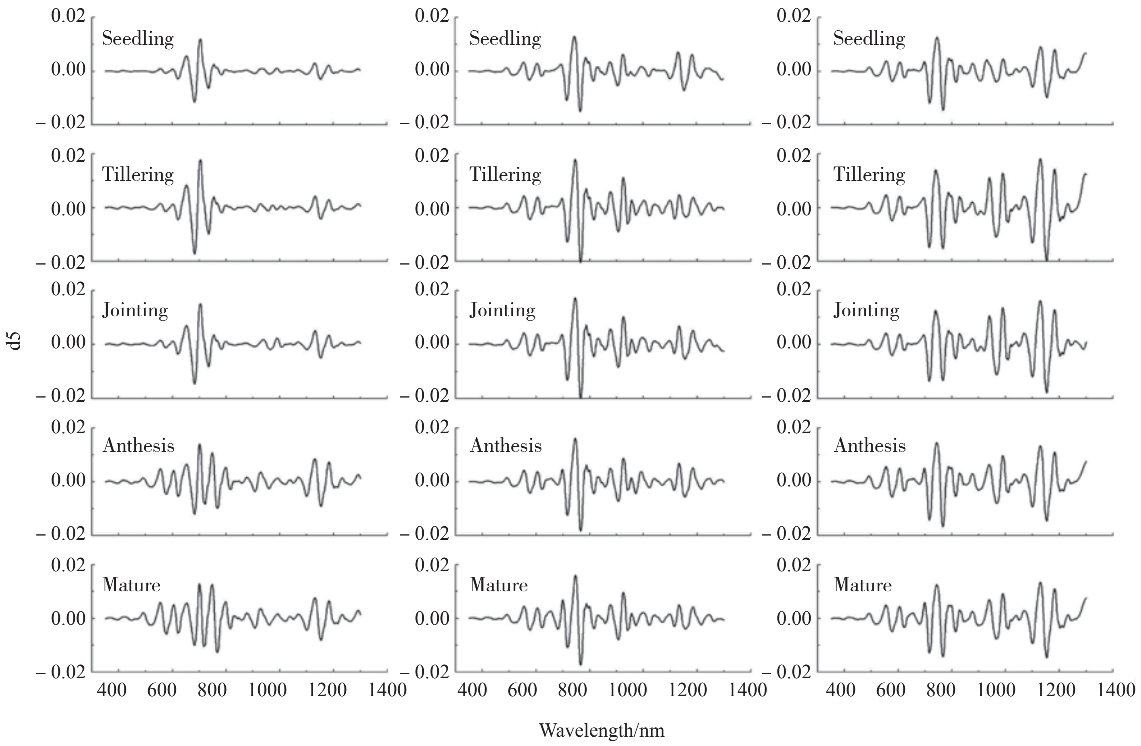

(a) (b) (c)

Fig.3 The d5 curve of rice with different pollution levels for each growth stage
(a) High pollution; (b) Medium pollution; (c) Low pollution

Table 3 The amplitude of singularity point and fractal dimension of d5 of rice with different heavy metal pollutions for each growth stage

Pollution level	Parameters	Growth stage				
		Seedling	Tillering	Jointing	Anthesis	Mature
High	Minimum /10^{-2}	–1.20	–1.72	–1.46	–1.30	–1.29
	Maximum /10^{-2}	1.20	1.78	1.50	1.39	1.20
	Singularity amplitude /10^{-2}	2.40	3.50	2.96	2.69	2.49
	Fractal dimension	1.151	1.191	1.202	1.235	1.261
Medium	Minimum /10^{-2}	–1.50	–2.04	–1.99	–1.83	–1.73
	Maximum /10^{-2}	1.29	1.79	1.72	1.61	1.59
	Singularity amplitude /10^{-2}	2.79	3.83	3.71	3.44	3.32
	Fractal dimension	1.249	1.259	1.261	1.265	1.274
Low	Minimum /10^{-2}	–1.45	–1.99	–1.78	–1.67	–1.46
	Maximum /10^{-2}	1.26	1.82	1.62	1.45	1.34
	Singularity amplitude /10^{-2}	2.71	3.81	3.40	3.12	2.80
	Fractal dimension	1.278	1.281	1.286	1.297	1.302

Note: Singularity amplitude =Maximum- minimum

3.3 Distinguishing high-frequency components of rice under Pb pollution

In order to examine whether high-frequency component of d5 was credible and extensive in distinguishing stress levels of rice under Pb pollution, 200 data sets from the tillering growth stage of rice with different levels of Pb pollution were randomly selected. The average value was calculated from 10 consecutive data sets and thus 20 groups spectral curve were obtained. 20 groups original reflectance of rice with differing Pb pollution in the regions between 350 nm and 1300 nm were performed by wavelet transform with 'Db5' wavelet function. Fig. 4 showed the original reflectance and d5 curve of rice with differing Pb pollution. As seen in Fig.4(a), reflectance spectra of rice with three levels of Pb pollution showed intersecting distribution tendency in 350 nm and 1300 nm, especially for reflectance spectra of rice with medium pollution. This indicates that original reflectance spectral is poor at differentiating the stress levels of rice with Pb pollution in a 'real world' agro-ecosystem. However, from Fig. 4(b), variety separation of d5 in rice with three levels of Pb pollution is clear, which indicates that the d5 from WT can provide diagnostic information to distinguish the spectral signal of rice with three levels of Pb pollution, especially for obvious separation occurred around 680 nm, 700 nm, 730 nm, 1120 nm, 1150 nm and 1180 nm. In addition, d5 of rice with equivalent level of Pb pollution was closely arranged. Obviously, three relatively independent clusters for d5 curves were exhibited in Fig. 4 (b). It can be interpreted that the equivalent level of heavy metal pollution have similar effect on the heavy metal diffusion in crops from soil and the difference of heavy metal content in crops occurred in different contaminated levels in soil.

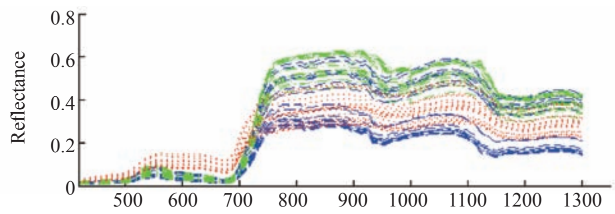

(a)

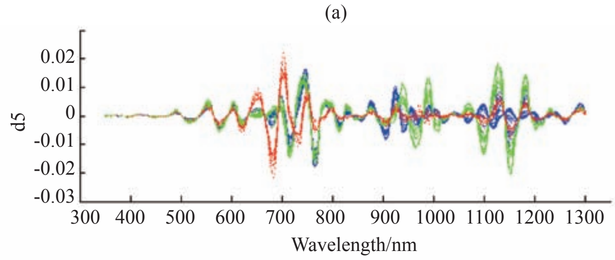

(b)

Fig. 4 The original reflectance and d5 curve of rice under different heavy metal pollution
(a) the original reflectance; (b) d5 curve

3.4 Analyzing fractal dimension of high-frequency of rice under different Pb pollution

To assess the effectiveness of the proposed method for fractal dimension of d5 in distinguishing stress levels of rice under Pb pollution, hyperspectral data was processed using wavelet transform in conjunction with fractal technology. Firstly, the d5 was obtained by performed wavelet transform to the average spectral reflectance. Secondly, the fractal dimension of d5 was calculated. Our previous analysis indicated that the best stage for monitoring heavy metal stress is at the tillering growth stage of rice (Liu, *et al*., 2010). Thus, fractal dimension of d5 in rice at tillering stage was calculated and analyzed (Fig. 5). As shown in Fig. 5, the obvious distinction of the fractal dimension of d5 was observed at rice under all three levels of Pb pollutions. At the same time, the close distribution tendency was displayed in the fractal dimension of d5 in rice with the equivalent level of Pb pollution in 2008 and 2009. It can be inferred that d5 of rice with three levels of Pb pollution was characterized by three closely clusters curve with relatively independent distribution tendency. In order to investigate whether the fractal dimension of d5 was a stable indicator for detecting the heavy metal induced-stress in crop in growing different years, annual variation rate was viewed as the parameter for assessing the stability of the fractal dimension of d5. Low values in annual variation rate indicates that fractal dimension of d5 is a very stable indicator. The equation of annual variation rate is as follows:

$$\alpha = D_{09} - D_{08} \quad (3)$$

$$\alpha' = \frac{|D_{09} - D_{08}|}{D_{08}} \times 100\% \quad (4)$$

where α and α' are the annual absolute variation rate and annual relative variation rate of fractal dimension respectively. D_{08} and D_{09} are fractal dimension of d5 in 2008 and 2009, respectively. Accurate statistics for fractal dimension of d5 are calculated in Table 4 according to the above equations. As seen in Table 4, the mean fractal dimension values of d5 in the rice samples are found in the order of $D_H < D_M < D_L$ (fractal dimension of d5 as high, medium and low pollution labeled as D_H, D_M, D_L respectively) for rice growing in 2008 and 2009. Generally speaking, the annual variation rate for fractal dimension values of d5 is low. In detail, on the one hand, according to the annual absolute variation rate, fractal dimension values of d5 of rice will either decrease or increase slightly. Namely, d5 of rice under high pollution and low pollution decrease slightly, while that of rice under medium pollution increases slightly. On the other hand, the annual relative variation rate for the fractal dimension values of d5 is lower than 4%. It can be concluded that the fractal dimension value of d5 is a stable indicator, and that it can eliminate the meteorological conditions on spectral reflectance of crops. As shown in Table 4, the annual relative variation rates for fractal dimension of d5 value in rice with high pollution and low pollution are slightly greater than that of rice with medium. The possible reason is that the effect of low or high Pb concentrations in soil on rice is relative stable. Specifically, low Pb concentrations in soil are of great benefit to rice and high Pb concentrations in soil will be harmful to rice and prevent rice from growing. However, if rice is contaminated by the medium Pb concentration in soil, the pigment, cell and physiological structure of rice are gradually stressed. And the effect of Pb concentration in soil on rice is dependent on the rice growing environmental conditions, such as temperature, light, water and so on.

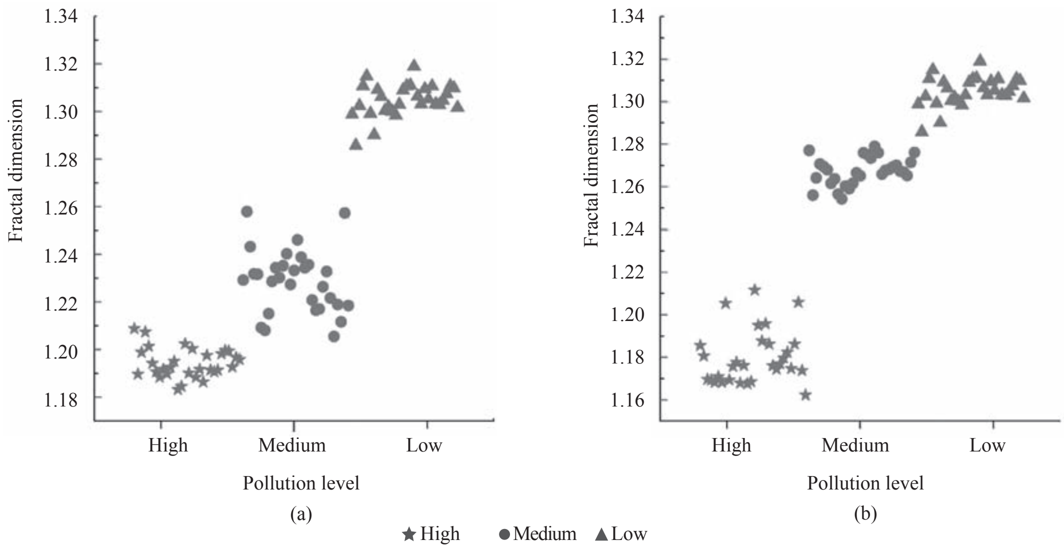

Fig. 5 The scatter map of fractal dimension for d5 curve of rice under different heavy metal pollution
(a) 2008 year; (b) 2009 year

Table 4 The statistics of fractal dimension for d5 curve of rice under different heavy metal pollution

Year	Parameter	High pollution	Medium pollution	Low pollution
2008	Range	1.183 – 1.209	1.206 – 1.258	1.286 – 1.319
	Mean	1.194	1.229	1.305
	Stdev	0.006	0.013	0.006
2009	Range	1.162 – 1.212	1.254 – 1.279	1.277 – 1.309
	Mean	1.179	1.267	1.293
	Stdev	0.013	0.006	0.010
Annual variation ratio*	Annual absolute variation ratio	– 0.015	0.038	– 0.012
	Annual relative variation ratio (%)	1.26	3.09	0.92

Note: *The variation of fractal dimension is based on rice in 2009 according to rice in 2008 as standard value

3.5 Relationship between fractal dimension of high-frequency components and stress levels of rice with heavy metal pollution

The three linguistic variables (High, medium and low) as stress levels were defined as fuzzy sets using high (lower) semi-trapezoidal functions from a set of given subsets of rice samples in 2008. The membership functions represent the degree to which the specified fractal dimension of d5 belongs to the fuzzy set. The membership degrees of assessment parameters at each class can be described quantitatively by a set of formulae comprised of membership functions as follows:

(i) The membership function of assessment fractal dimension of d5 for rice with high pollution can be described quantitatively as :

$$u(D_i)=\begin{cases}1 & D_i\leqslant 1.200\\ \dfrac{1.220-D_i}{1.220-1.200} & 1.200<D_i<1.220\\ 0 & D_i>1.220\end{cases} \quad (5)$$

(ii) The membership function of assessment fractal dimension of d5 for rice with medium pollution can be described quantitatively as :

$$u(D_i)=\begin{cases}\dfrac{D_i-1.200}{1.220-1.200} & 1.200<D_i<1.220\\ 1 & 1.220\leqslant D_i\leqslant 1.275\\ \dfrac{1.280-D_i}{1.280-1.275} & 1.275<D_i<1.280\\ 0 & D_i<1.200,\ D_i>1.280\end{cases} \quad (6)$$

(iii) The membership function of assessment fractal dimension of d5 for rice with low pollution can be described quantitatively as :

$$u(D_i)=\begin{cases}0 & D_i\leqslant 1.275\\ \dfrac{D_i-1.275}{1.280-1.275} & 1.275<D_i<1.280\\ 1 & D_i\geqslant 1.280\end{cases} \quad (7)$$

To examine whether established model has the stable performance of predictions for stress levels of rice under heavy metal pollution, experiments were then conducted to verify the accuracy of the fuzzy logic model. The correct classification ratio was measured by dataset from 2009. Experimental results are shown in Table 5. From Table 5, it can be seen that high accuracy was obtained from the fuzzy logic model with 93.33% accuracy for high pollution, 93.33% accuracy for medium pollution and 96.67% for low pollution. It suggests that fuzzy logic model can work well in monitoring the stress levels of rice under Pb pollution with high accuracy of the predicted stress levels through semi-trapezoidal functions for the respective stress levels of rice under Pb pollution.

Furthermore, the frequency histograms for rice under different levels of heavy metal pollution in 2008 and 2009 were shown in Fig. 6. As seen in Fig. 6 (a) (b) (c), fractal dimension values of d5 for rice samples under high, medium and low pollution were 86.7% between 1.160 and 1.200, 75% between 1.220 and 1.275, 91.7% between 1.280 and 1.320, respectively. The general distribution in 2008 and 2009 for fractal dimension values of rice under heavy metal pollution were shown in Fig. 6 (d), and fractal dimension values of d5 for rice samples under three pollution levels lacked of clear boundary with interaction regions. Namely, rice under high and medium pollution has a uniform region with fractal dimension values of d5 between 1.220 and 1.220. Similarly, rice under medium and low have a uniform region with fractal dimension values of d5 between 1.275 and 1.280. Based on the above analysis, it is suitable for fuzzy logic model to solve the uncertainty and fuzzy problems, such as crop under heavy metal pollution. Since membership function on the basis of fuzzy model could provide a comprehensive and operational method to assess stress levels of rice under heavy metal pollution and the evaluation results are reasonable and credible.

Table 5 The verification of fuzzy logic model for rice with different pollution levels

Experimental sites	Sample	Measured pollution level	Predicated result		Classification accuracy
			Pollution level	Sample	
A	30	High	High	28	93.33%
			Medium	2	
			Low	0	
B	30	Medium	High	0	93.33%
			Medium	28	
			Low	2	
C	30	Low	High	0	96.67%
			Medium	1	
			Low	29	

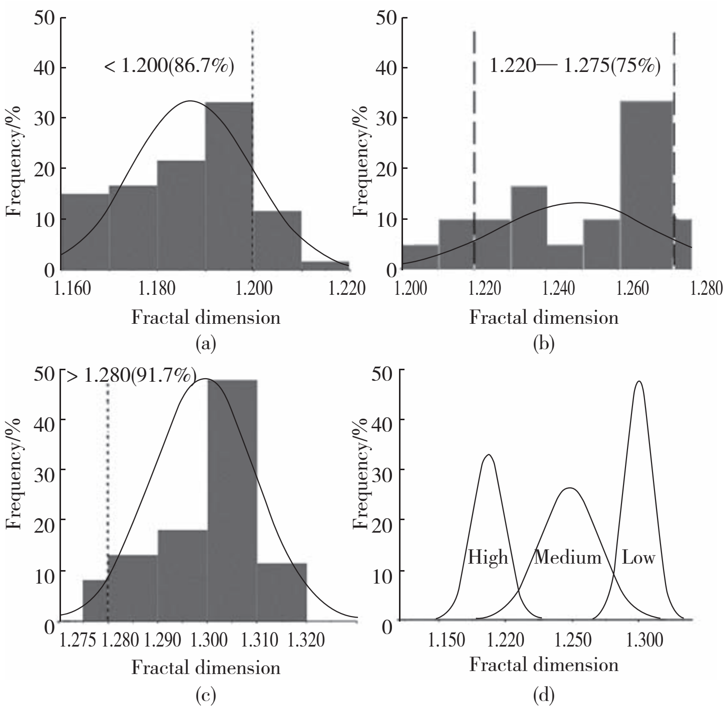

Fig. 6 The frequency distribution for d5 curve of rice under different heavy metal pollution
(a) High pollution; (b) Medium pollution; (c) Low pollution; (d) Three pollution levels

4 RESULTS AND DISCUSSIONS

(1) The fifth high-frequency component (d5) of rice can effectively detect the subtle spectral characteristic information related to heavy metal pollution and discriminate different stress levels of rice under heavy metal pollution. This is because that wavelet transform to spectral reflectance can succeed both in removing the non-spectral scattering effects and eliminating the environmental conditions (such as light, temperature, moisture and other meteorological conditions) on spectral reflectance of crops. It suggests that wavelet transform appears to be very promising in removing noises and amplifying the subtle spectral characteristic information associated with various environmental stresses. Compared with the traditional derivative transform, original reflectance or vegetation indices (Liu, *et al*., 2006; Li, *et al*., 2008; Chi, *et al*., 2009), wavelet transform have a particular advantage in detecting stress levels of crop under heavy metal pollutions. The two primary advantages are as follows. First, it is suitable for hyperspectral high-frequency component after performing wavelet transform to reflectance to detect the stress information in both high-polluted crop and crop growing in natural agro-ecosystems with relative low level of pollutants. In addition, wavelet transform technology can be widely used to detect spectral singularity information and amplify subtle spectral characteristic information of crop under various environmental stresses. Second, wavelet transform has the ability for wavebands localization in abnormal phenomenon of spectral reflectance of metal-induced crops. Thereby, it is conductive to investigate the distinction of spectrum among crop under different heavy metal pollution.

(2) When rice is polluted by heavy metal, the subtle differences in spectral reflectance occur at rice growing at different growth stages. Such difference can be disclosed by the fractal dimension values of d5. In 2008 and 2009, the annual relative variation rate for the fractal dimension values of d5 is lower than 4%. While the classification accuracy for three stress levels of rice under Pb pollution are all above 75%. Namely, fractal dimension values of d5 for rice samples under high, medium and low pollution are 86.7% between 1.160, 1.200, 75% between 1.220 and 1.275, 91.7% between 1.280 and 1.320, respectively. It indicates that the fractal dimension of d5 is a stable and sensitive indicator for identifying the stress levels of crop. The mainly two reasons are as follows. Firstly, after original reflectance is performed by wavelet transform, d5 succeeds both in removing the non-spectral scattering effects and in amplifying the stress information related to heavy metal pollution together with wavebands localizations. Secondly, fractal dimensions of d5 in the 350—1300 nm can be used to explain the comprehensive variations of spectrum curves as a ‘global parameter’, and it has the advantage of capturing more information provided by reflectance spectra than previous analytical approaches such as single-band or some spectral vegetation indices for investigating changes in plant stress (Kemper&Sommer, 2002; Slonecker, *et al*., 2009).

(3) The relationship between the fractal dimension of d5 and stress levels of rice Pb pollution are constructed by using high (low) semi-trapezoidal functions. When it comes to the fractal dimension values of d5 located at the two overlap regions between 1.200 and 1.220, between 1.275 and 1.280, membership functions succeeds in dealing with such problem because the specified fractal dimension of d5 belongs to the fuzzy set, namely, high pollution, medium or low pollutions. The membership degree can effectively describe the status of gradual change in stress levels of crops. In addition, it can be expected to solve many problems with uncertainties, randomness and fuzziness. Therefore, the membership functions are served as useful tools to solve the fuzzy problems, such as stress levels of crop under environmental conditions.

In summary, wavelet transform, fractal analysis in conjunction with fuzzy mathematics can effectively detect the stress levels of rice by extracting, calculating and modeling subtle spectral characteristic information associated with heavy metal pollutions. Yet it should be noted that constructed models will need revisions according to different crop types and sources of pollutants, when membership functions based on the fractal dimension of high-frequency components and stress levels are used to assess the stress levels of crop under heavy metal pollution in other environmental conditions. The proposed model can be applied to ground hyperspectral data as well as spaceborne or airborne hyperspectral imagery through the atmospheric corrections.

REFERENCES

Borodich F M. 1997. Some fractal models of fracture. *Journal of the Mechanics and Physics of Solids*, **45**(2): 239–259

Chen S N, Liu X H, Hou J, Liu X H, Chi G Y, Cui B S and Yang Z F. 2007. Study on the spectrum response of *Brassica Campestris* L. leaf to the zinc pollution. *Spectroscopy and Spectral Analysis*, **27**(9): 1797–1801

Chi G Y, Chen X, Shi Y and Liu X H. 2009. Spectral response of rice (*Oryza sativa* L.) leaves to Fe^{2+} stress. *Science in China Series C-Life Sciences*, **52**(8): 747–753

Choe E, van der Meer F, van Ruitenbeek F, van der Werff H, de Smeth B and Kim Y W. 2008. Mapping of heavy metal pollution in stream sediments using combined geochemistry, field spectroscopy, and hyperspectral remote sensing: a case study of the Rodalquilar mining area, SE Spain. *Remote Sensing of Environment*, **112**(7): 3222–3233

Clevers J G P W, Kooistra L and Salas E A L. 2004. Study of heavy metal contamination in river floodplains using the red–edge position in spectroscopic data. *International Journal of Remote Sensing*, **25**(19): 3883–3895

Collins W, Chang S H, Raines G L, Canney F and Ashley R. 1983. Airborne biogeophysical mapping of hidden mineral deposits. *Economic Geology*, **78**(4): 737–749

Daubechies I. 1990. The wavelet transform, time-frequency localization and signal analysis. *IEEE Transactions on Information Theory*, **36**(5): 961–1005

Du H Q, Jin W, Ge H J, Fan W Y and Xu X J. 2009. Using fractal dimensions of hyperspectral curves to analyze the healthy status of vegetation. *Spectroscopy and Spectral Analysis*, **29**(8): 2136–2140

Dunagan S C, Gilmore M S and Varekamp J C. 2007. Effects of mercury on visible/ near-Infrared reflectance spectra of mustard spinach plants (*Brassica rapa* P.). *Environmental Pollution*, **148**(1): 301–311

Guan L and Liu X N. 2009. Experimental research on remote sensing diagnosis method of Cd pollution stress in rice. *Transactions of the Chinese Society of Agricultural Engineering*, **25**(6): 168–173

Kemper T and Sommer S. 2002. Estimate of heavy metal contamination in soils after a mining accident using reflectance spectroscopy. *Environmental Science and Technology*, **36**(12): 2742–2747

Kooistra L, Salas E A L, Clevers J G P W, Wehrens R, Leuven R S E W. Nienhuis P H and Buydens L M C. 2004. Exploring field vegetation reflectance as an indicator of soil con tamination in river floodplains. *Environmental Pollution*, **127**(2): 281–290

Kooistra L, Wehrens R, Leuven R S E W and Buydens L M C. 2001. Possibilities of visible-near-infrared spectroscopy for the assessment of soil contamination in river floodplains. *Analytica Chimica Acta*, **446**(1–2): 97–105

Li Q T, Yang F J, Zhang B , Zhang X and Zhou G Z. 2008. Biogeochemistry responses and spectral characteristics of Rhus Chinensis Mill under heavy metal. *Journal of remote sensing*, **12**(2): 284–290

Liu M L, Liu X N, Li T and Xiu L N. 2010. Analysis of hyperspectral singularity of rice under Zn pollution stress. *Transactions of the Chinese Society of Agricultural Engineering*, **26**(3): 191–197

Liu S H, Liu X H, Hou J, Chi G Y and Cui B S. 2007. Study on the spectral response of *Brassica Campestris* L. leaf to the copper pollution. *Science in China Series E: Technological Sciences*, **37**(5): 693–699

Montzka C, Canty M, Kreins P, Kreins P, Kunkel R, Menz G, Vereecken H and Wendland F. 2008. Multispectral remotely sensed data in modelling the annual variability of nitrate concentrations in the leachate. *Environment modeling and software*, **23**(8): 1070–1081

Noh H, Zhang Q, Shin B, Han S and Feng L. 2006. A neural network model of maize crop nitrogen stress assessment for a multi-spectral imaging sensor. *Biosystems Engineering*, **94**(4): 477–485

Osborne S L, Schepers J S, Francis D D and Schlemmerb M R. 2002. Detection of phosphorus and nitrogen deficiencies in corn using spectral radiance measurements. *Agronomy Journal*, **94**(6): 1215–1221

Qi Y B, Huang B, Derlek J L and Wang Z G. 2008. Comparison of heavy metal fractions distribution in paddy soil under anoxic and oxidized conditions. *Ecology and Environment*, **17**(6): 2228–2233

Ren H Y, Zhuang D F, Pan J J, Shi X Z and Wang H J. 2008. Hyperspectral remote sensing to monitor vegetation stress. *Journal of Soils and Sediments*, **8**(5): 323–326

Schuerger A C , Capelle G A , Di Benedetto J A , Mao C Y, Thai C N, Evans M D, Richards J T, Blank T A and Stryjewski E C. 2003. Comparison of two hyper-spectral imaging and two laser-induced fluorescence instruments for the detection of zinc stress and chlorophyll concentration in bahia grass (*Paspalum notatum* Flugge.). *Remote Sensing of Environment*, **84**(4): 572–588

Slonecker T, Haack B and Price S. 2009. Spectroscopic analysis of arsenic uptake in pteris ferns. Remote Sensing. DOI: 10.3390/rs1040644

van der Meer F. 2006. Indicator kriging applied to absorption band analysis in hyperspectral imagery: a case study from the Rodalquilar epithermal gold mining area, SE Spain. *International Journal of Applied Earth Observation and Geoinformation*, **8**(1): 61–72

Wang L, Lin Q Z, Jia D, Shi H S and Huang X H. 2007. Study on the prediction of soil heavy metal elements content based on reflectance spectra. *Journal of remote sensing*, **11**(6): 906–913

Wang M Q and Zhang M K. 2002. Concentrations and chemical associations of heavy metals in urban and suburban soils of the Hangzhou City, Zhejiang Province. *Acta Scientiae Circumstantiae*, **22**(5): 603– 608

Zhao Q G, Zhou B Z and Yang H. 2002a. Studying on environmental quality and agricultural safety problem in Jiangsu Province. *Soil*, **34**(1): 1–8

Zhao Q G, Zhou B Z, Yang H, Liu S L. 2002b. Some considerations on safety of arable land resources in China: problems and countermeasures. *Soil*, **34**(6): 293–302

基于高光谱高频组份分形特征的水稻铅胁迫评估

刘美玲，刘湘南，曹仕，李婷，吴伶

中国地质大学（北京）信息工程学院，北京 100083

摘　要：通过研究铅污染胁迫下水稻的光谱高频组份的分维数来诊断水稻铅污染胁迫水平。根据实验区水稻冠层实测ASD高光谱数据和同步获取的农田土壤重金属含量数据，利用Daubechies小波系中的“Db5”母小波对水稻的350—1300 nm波段范围进行小波分解得到第5层高频组份(d5)，并采用盒维法计算d5的分维数，最后采用模糊数学建立d5的分维数与污染胁迫水平的数学模型。结果表明：d5能有效地探测到铅污染胁迫的光谱弱信息，并实现不同污染水平水稻高光谱信号的分离；d5分维数在同一污染水平的年际相对变化率小于4%，不同污染水平的区分度大于75%，即高、中和低污染水平水稻高光谱d5分维数的86.7%、75%和91.7% 分别集中在1.160—1.200，1.220—1.275和1.280—1.320三个区间；采用升(降)半梯形分布的隶属度函数建立水稻高光谱d5分维数与其污染胁迫水平的数学模型，并进行了模型精度检验，其判别精度大于90%。小波变换、分形分析和模糊数学三者相结合有效地实现了光谱弱信息提取、度量及建模，达到水稻重金属污染胁迫状况监测的目的，也为作物其他环境胁迫弱信息的动态识别与精确度量提供借鉴意义。

关键词：高光谱遥感，小波变换，分形分析，隶属度函数，水稻，铅污染胁迫

中图分类号：S127　　**文献标志码**：A

引用格式：刘美玲，刘湘南，曹仕，李婷，吴伶．2011．基于高光谱高频组份分形特征的水稻铅胁迫评估．遥感学报，**15**(4): 811–830
Liu M L, Liu X N, Cao S, Li T and Wu L. 2011. Assessment of Pb-induced stress levels on rice based on fractal characteristic of spectral high-frequency components. *Journal of Remote Sensing*, **15**(4): 811–830

1　引　言

农田重金属污染具有毒性大、隐蔽性强和生态效应复杂等特点，是当今世界面临的重大生态环境问题之一(王美青和章明奎，2002；齐雁冰 等，2008)。据报道，中国受重金属污染的土壤面积已达2000万hm^2，占耕地总面积的1/6(赵其国 等，2002a)。江苏省粮食(水稻、小麦)中铅含量超标(国家卫生标准)率为21.4%，局部地区超标率达66%(赵其国 等，2002b)。由于经济的快速发展和环保措施的相对滞后，中国土壤重金属污染出现愈演愈烈的趋势。如何快速有效地监测农田重金属污染对于环境保护和粮食安全具有重要意义。利用高光谱遥感对作物重金属污染现状、动态过程及发展趋势进行监测、模拟和评估已成为热点研究领域之一(Kooistra 等，2001；Osborne 等，2002；Dunagan 等，2007；Montzka 等，2008)。高光谱遥感所提供的精细光谱可有效地分析作物叶片的生化成分，因而可以大面积、快速、无损识别与度量作物重金属污染状况。国内外学者利用受污染胁迫的植被敏感因子(如叶绿素、营养元素等生化成分)变化的高光谱响应特征揭示植被污染水平已经取得了一些研究成果，Choe等人利用传统地球化学分析和高光谱遥感相结合的方法展开矿区污染情况调查(Choe 等，2008；李庆亭 等，2008)，Clevers等人利用高光谱植被指数及红边位置监测河漫滩土壤的重金属污染状况(Clevers 等，2004；Kooistra 等，2004)，认为重金属在某些波段的光谱特征参数可以作为污染现状监测的有效指标。此外，一些学者研究在实验室控制条件下重金属对盆栽作物光谱特征变化的影响，Collins等人对高粱、芥菜和蕨类等作物在

收稿日期：2010-04-22；**修订日期**：2010-08-20
基金项目：国家自然科学基金项目(编号：40771155)；国家高技术研究发展计划(863计划)专项经费(编号：2007AA12Z174)
第一作者简介：刘美玲(1978—　)，女，博士，主要从事遥感信息分析与地学应用研究。E-mail: liumeiling427@126.com。
通信作者：刘湘南，liuxncugb@163.com。

实验室人为控制添加不同剂量的Cu，Pb，Zn和As等重金属污染条件下的叶绿素吸收谷和红边等光谱特征变化进行研究(Collins 等，1983；Schuerger 等，2003；Slonecker 等，2009)，刘素红等人研究人为控制条件下Cu、Zn和Pb分别对小麦、白菜和水稻光谱反射特征的影响(刘素红 等，2006；陈思宁 等，2007；Ren 等，2008)，结果表明，“红边”蓝移程度及近红外反射坪的变化幅度与作物体内的叶绿素含量和重金属含量均存在较强的相关关系。上述研究表明，高浓度污染胁迫由于引起了植被生理生态参数的一些变化，从而导致光谱反射率发生较为显著地变化(如“红边”蓝移，叶绿素吸收谷变浅以及近红外反射坪降低)，但生长在“自然农田生态系统”的作物遭受相对较低污染水平胁迫条件下其生理生态参数的变化通常较小，在原始高光谱曲线上一般不会出现显著和稳定的响应特征，同时影响光谱变化的因素很多，污染胁迫导致的微小变化对光谱变化产生的贡献一般不易甄别，需采用有效的光谱分析方法提取和增强污染胁迫的光谱弱效应。一些研究者采用吸收特征光谱参数、多维光谱指数表达空间、人工神经网络模型或分形分维数等对原始光谱信息进行变换或增强的技术提取诊断光谱指数，对植被污染胁迫状况进行识别和评价(van der Meer，2006；Noh 等，2006；王璐 等，2006；关丽和刘湘南，2009；杜华强 等，2009)。然而作物污染胁迫遥感信息是一种大面积内微小变化量的弱信息，具有随机性和不确定性，仅仅使用一些简单和单一的光谱分析方法难于提取作物污染胁迫响应的光谱弱信息特征。本文尝试利用小波变换、分形分析和模糊数学3者相结合的方法对水稻重金属污染胁迫水平进行分析和评价，旨在对大面积范围内微小变化量的光谱弱效应进行增强、计算和建模，从而实现大面积作物铅污染动态监测。

2 材料与方法

2.1 样区设计与数据采集

选取江苏省苏州市东桥和正仪等3个铅污染水平各不相同的农田样地作为实验区，即高污染区A号采样地，中污染区B号采样地和低污染区C号采样地。实验区种植的作物为水稻，品种为常优一号，A、B、C三号样地水肥供应和气象条件基本一致，管理措施同当地水稻常规管理。该区处于平原地带，属亚热带季风气候，水热充沛，年平均降水量1094 mm，年平均气温15.7℃，年光照时数1965 h，土壤以黄褐土为主，pH值约为6.2，有机质含量约为3%。农田土壤的主要重金属含量如表1所示。

本研究的实验数据来源于2008年和2009年两年大田水稻实验。光谱反射率采用美国ASD公司生产的FieldSpec光谱仪对水稻进行测定，测定前用标准白板进行校正，视场角为10°，波段范围为350—2500 nm，在水稻生长期间共进行5次测量，测量时期包括出苗期、分蘖期、拔节期、开花期和成熟期，光谱测试各个生长期取30—40个测点，分别进行编号，每个点测10次。然后对测试点区域的水稻和土壤进行同步采样，分别用样品袋和土壤盒保存送至实验室分析化验，重金属含量(Cu、Zn、Pb、Cr、As、Cd)采用原子吸收法测定。

表1 实验区农田土壤重金属含量

实验样区	地理坐标		As	Cr	Cu	Zn	Pb	Cd	污染水平
		背景值*Ci*	13.6	62.6	24.4	80.1	29.1	0.065	
A	31° 25' N, 120° 31' E	平均值*Si*	8.90	54.2	23.8	78.5	128.3	0.097	高
		污染指数*Pi*	0.65	0.87	0.98	0.98	4.41	1.49	
B	31° 24' N, 120° 33' E	平均值*Si*	7.20	60.5	22.3	59.3	71.7	0.082	中
		污染指数*Pi*	0.53	0.97	0.91	0.74	2.46	1.26	
C	31° 21' N, 120° 51' E	平均值*Si*	6.50	61.4	23.9	37.4	30.8	0.04	低
		污染指数*Pi*	0.48	0.98	0.98	0.47	1.05	0.66	

注：*Ci*为土壤重金属元素背景值(参考中国环境监测总站)，*Si*为实测重金属浓度，*Pi*=*Ci*/*Si*，低污染(*Pi*=1–2)；中度污染(*Pi*=2–3)；高污染(*Pi*>3)。

2.2 方法

为了对水稻重金属污染胁迫光谱弱效应进行有效地增强和探测，本研究使用小波变换、分形分析及模糊数学3者相结合的方法，其流程如图1所示，主要分为3个步骤：(1)多尺度小波变换获得高光谱高频组份，以提取和增强重金属污染胁迫弱信息；(2)分形分析对水稻重金属污染胁迫弱信息进行分维数D的定量计算；(3)模糊隶属度函数建立分维数与胁迫水平的数学模型。通过小波变换去噪和探测奇异信号的功能达到提取和增强重金属污染胁迫弱信息的目的，具体操作步骤先选取第5层高频组份d5，然后采用分形技术对d5进行分维数(D)的计算以获取光谱定量参数，最后采用模糊数学中的隶属度函数建立定量光谱参数D与胁迫水平之间的数学模型。

2.2.1 小波变换提取光谱高频组份

小波变换是用一簇函数去逼近待分析的信号，它适合探测信号的奇异性。奇异性是指函数在某处有间断点或某阶导数不连续(Daubechies，1990)。目前用于小波分析的函数有很多，不同的信号处理问题选用的小波函数有所不同。试验结果表明Daubechies小波系中的“Db5”小波函数对重金属污染胁迫下的水稻光谱异常信号探测有较好的性能(刘美玲 等，2010)。处理过程是两个互补对称滤波器将原始信号分解为低频和高频2部分，然后继续用同样的处理方法对信号的低频部分进行再分解，经过多层分解可以将原始信号分解为多个子信号，公式如下：

$$f(\lambda)=a_j(\lambda)+\sum_{i=1}^{j}d_i(\lambda) \tag{1}$$

式中，$f(\lambda)$为光谱原始信号，j为分解层，a_j为低频部分，d_i为高频部分。其中低频信号(信号较平稳)具有较高的频率分辨率和较低的波段分辨率，反映了光谱信号的总体特征，而在高频部分具有较高的波段分辨率和较低的频率分辨率，反映信号的细节特征，很适合于探测正常光谱信号中夹带的瞬态异常现象。本文将原始光谱反射率的350—1300 nm波段光谱信号分为不同数目的层，发现将信号分为5层可以达到本研究对信号处理的目的。光谱信号经5层小波分解得到低频部分a5和高频部分d1，d2，d3，d4和d5(图1)，高频部分的d1，d2，d3和d4都含有较多的噪声信息，而d5既有效地去除了噪声又完整地保持了信号的奇异性，也就表明高频组份d5能探测到光谱信号中携带与污染胁迫水平相关的异常现象。

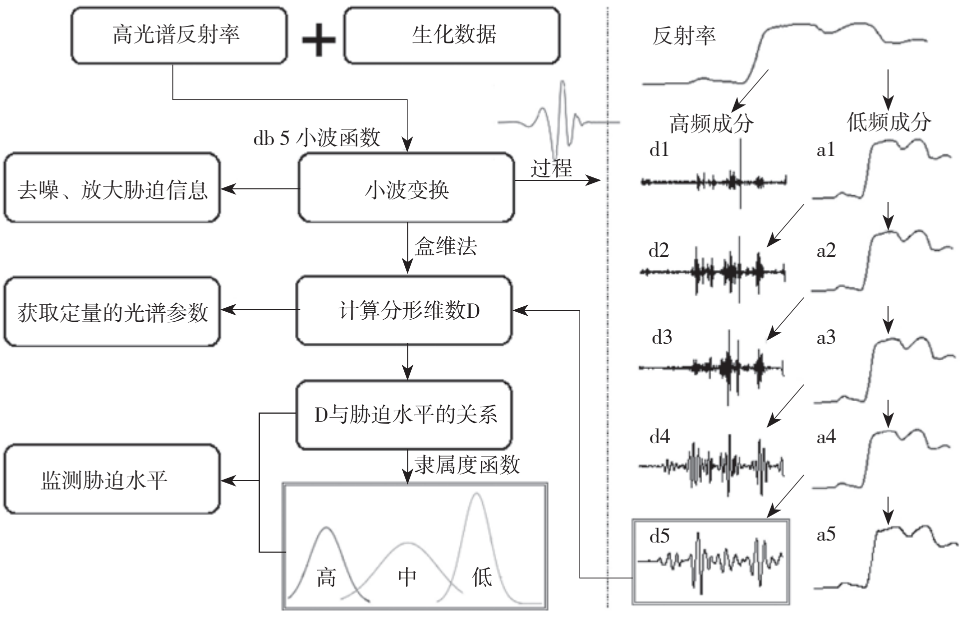

图1 重金属污染胁迫弱信息提取、计算和建模的技术路线

2.2.2 光谱高频组份的分维数计算

分形维数反映分形集的复杂性、不平度或卷积度，可以作为波形识别的一种特征度量。已有研究表明高光谱反射率具有分形特征(杜华强 等，2009)，d5作为光谱信号的变换形式，它同样具有分形特征。为了能全面而准确地对不同铅污染水平

的光谱弱信息进行量化和比较，本文采用分形技术来计算高频组份d5的分维数，这主要有两个方面的原因：第一，分形分析与小波变换在信号的“尺度变换”和“自相似性”两个方面存在着本质的一致性；第二，分维数能反映污染胁迫引起的光谱奇异性的“整体变化”，能捕捉到更多的光谱弱信息，从而提高光谱参数对胁迫水平反应的灵敏性。常用的分形维数计算方法有盒子维数、信息维数和Hausdorff维数等，本研究采用盒维法来计算分维数D(Borodich，1997)，其计算公式如下：

$$D = \lim_{n \to \infty} \frac{\log_2 M(n)}{\log_2 n} \tag{2}$$

式中，D是分维数；$M(n)$是奇异范围内的单位为1的网格数；n是曲线的分解尺度。

2.2.3 分维数与胁迫水平间隶属度函数的建立

模糊数学常常作为研究和处理具有“模糊性”现象问题的数学工具。由于水稻生理生化特征高光谱响应机理问题本身的复杂性，使得重金属污染胁迫的水稻光谱响应更复杂，此外胁迫水平评定等级划分的界限也是模糊的，没有一个确定的等级边界，因而本文采用模糊集理论中的隶属函数来表征作物重金属胁迫水平，以消除作物胁迫水平分级中的主观因素。隶属函数的确定有多种方式，常用的隶属度函数包括升(降)半阶隶属度函数、高斯隶属度函数和三角隶属度函数等。本文选用升(降)半梯形分布，建立一元线性隶属函数，根据d5分维数的实测值和各级评价标准计算出其分维数相对于各胁迫水平等级的隶属度，从而判断d5分维数与各作物胁迫水平等级之间的关系。

3 结 果

3.1 高频组份的分形特征对水稻铅污染胁迫的响应机理

在作物光谱曲线上，由于活跃的原子或离子官能团的电子跃迁或振动在某些特定的波段会形成吸收光谱特征(如叶绿素吸收谷)，这些吸收特征光谱引起了光谱信号的不连续，从而导致了光谱的奇异性。水稻受到铅污染胁迫时，重金属铅原子或离子进入水稻体内破坏其体内的分子环境，从而使得光谱本身奇异点(突变点)的位移和振幅产生变化，而这些奇异点在原始光谱信号上很难被察觉。如何探测到光谱信号的奇异点对于提取作物重金属胁迫产生的光谱弱效应是至关重要的。小波变换的时域-频域局部性质，对这种光谱信号奇异点出现的时刻能作定量地计算和分析(图2)。由图2可见，不同污染水平的光谱奇异点位置和幅度存在着差异，这种差异可以作为重金属污染水平的判别依据。以低污染水平的奇异点为标准，对高污染水平和中污染水平的奇异点发生的位移和相对变化幅度进行了统计(表2)。由表2可知，高污染和中污染水平奇异点的位移和幅度均发生了不同程度地改变，在696—788 nm 波段范围内奇异点位置发生了较大的改变，在876—1183 nm波段范围内奇异点幅度发生了较大改变。为全面地刻画不同污染水平的水稻由于受到铅污染胁迫所导致的奇异点的位移和振幅的整体变化情况，利用分形特征来描述波形的细微变化。对图2中d5的分维数进行计算，得到高、中和低污染水平的分维数分别是1.232，1.267和1.290，即分维数越低，污染胁迫水平越高。

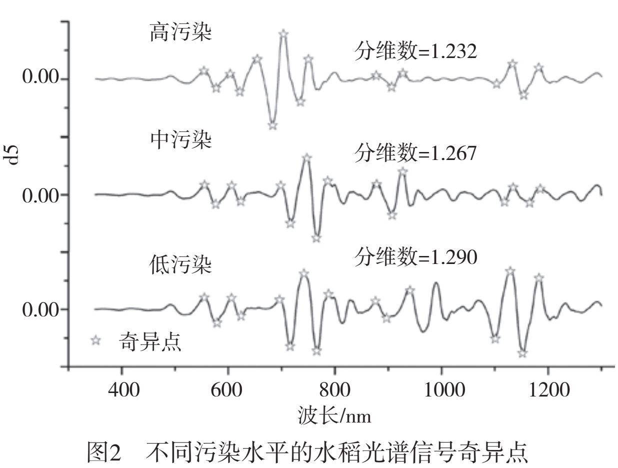

图2 不同污染水平的水稻光谱信号奇异点

表2 不同污染水平的水稻光谱奇异点位移和幅度

污染水平*	低污染水平奇异点位置	555	579	606	624	696	716	742	766	788	876	897	941	1101	1129	1152	1183
高–低	位移/nm	–1	–2	–3	–3	–42	–33	–39	–31	–38	1	9	–1	–2	–3	–3	–42
	幅度/%	32	34	56	91	106	25	26	46	31	57	10	69	83	61	64	64
中–低	位移/nm	0	–3	0	–1	2	0	5	–1	–2	2	10	–14	17	5	13	2
	幅度/%	20	30	21	0	6	22	2	4	10	29	129	22	76	81	82	81

*高污染水平和中污染水平分别相对于低污染水平，幅度=$|a-b|/|b|$，b为低污染水平奇异点位置所对应的d5值，a为高或中污染水平奇异点位置所对应的d5值。

3.2 不同生长期水稻高光谱高频特征分析

为分析不同生长期水稻高光谱高频组份的特性，在不同污染水平试验区水稻的出苗期、分蘖期、拔节期、开花期和成熟期等生长期随机选择200条高光谱数据求其平均，随后利用“Db5”小波函数对各时期平均反射率光谱曲线进行第5层小波分解(图3)。图3是高、中和低3个污染水平水稻各生长期的高光谱d5曲线，由图3可见，高污染水平的水稻d5曲线在不同生长期变化较显著，从出苗期至成熟期极值点数目逐渐增加，曲线变得越来越复杂。表3是采用奇异幅度和分维数对d5曲线在水稻不同时期的变化情况作定量计算，从表3可知，无论是高、中和低污染，奇异幅度从出苗期到分蘖期均迅速增加，并达到最大值，在随后的分蘖期→拔节期→开花期→成熟期，奇异幅度开始逐渐减少；奇异幅度在水稻的分蘖期处于最大值，可以认为是水稻在分蘖期生长旺盛，对重金属吸收机能最强所致，因而分蘖期可以作为探测水稻重金属胁迫的最佳时期。而分维数从出苗期→分蘖期→拔节期→开花期→成熟期均逐渐增加；分维数的这种变化规律可能是由于水稻在生长过程中，对铅不断地产生代谢作用使得光谱信号的突变点越来越多，导致曲线变得越来越复杂从而使分维数逐渐增大。

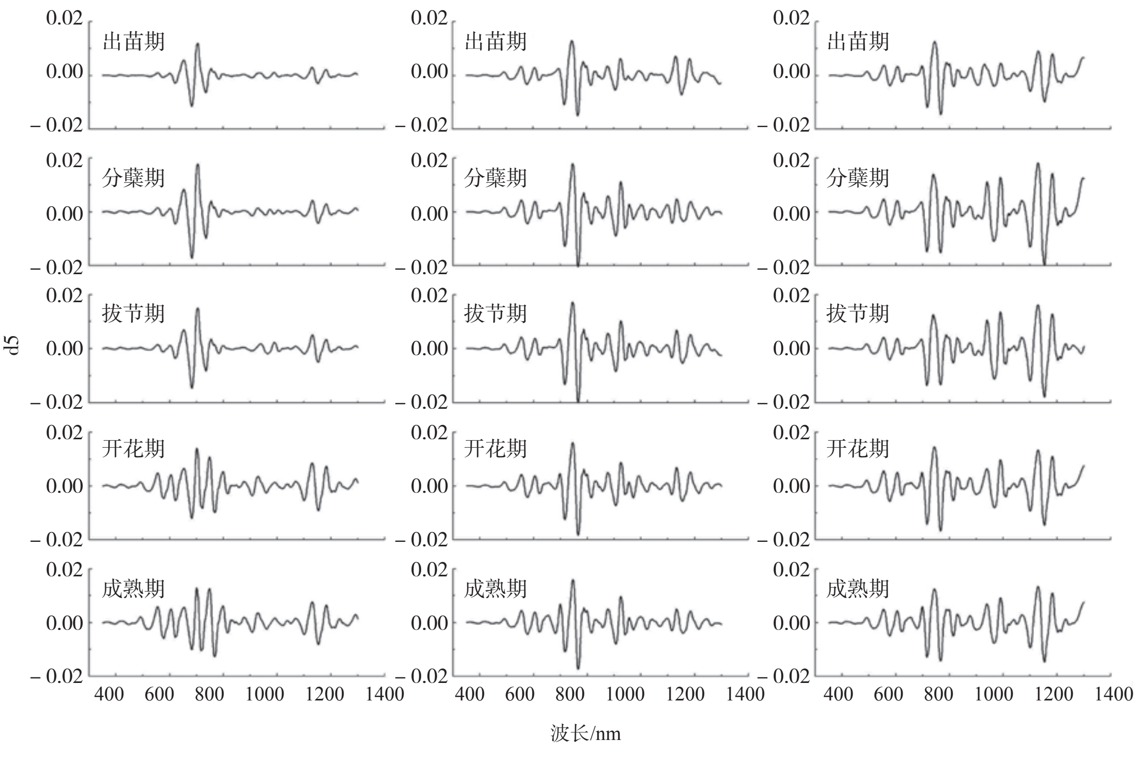

图3 不同污染水平的水稻各个生长期的d5曲线

(a)高污染；(b)中污染；(c)低污染

表3 不同污染水平的水稻各个生长期的奇异点幅度和分维数

污染水平	参数	生长期				
		出苗期	分蘖期	拔节期	开花期	成熟期
高	最小值/10^{-2}	−1.20	−1.72	−1.46	−1.30	−1.29
	最大值/10^{-2}	1.20	1.78	1.50	1.39	1.20
	奇异幅度/10^{-2}	2.40	3.50	2.96	2.69	2.49
	分维数	1.151	1.191	1.202	1.235	1.261
中	最小值/10^{-2}	−1.50	−2.04	−1.99	−1.83	−1.73
	最大值/10^{-2}	1.29	1.79	1.72	1.61	1.59
	奇异幅度/10^{-2}	2.79	3.83	3.71	3.44	3.32
	分维数	1.249	1.259	1.261	1.265	1.274

续表

污染水平	参数	生长期				
		出苗期	分蘖期	拔节期	开花期	成熟期
低	最小值/10^{-2}	−1.45	−1.99	−1.78	−1.67	−1.46
	最大值/10^{-2}	1.26	1.82	1.62	1.45	1.34
	奇异幅度/10^{-2}	2.71	3.81	3.40	3.12	2.80
	分维数	1.278	1.281	1.286	1.297	1.302

注：奇异幅度=最大值−最小值

3.3 不同铅污染胁迫水平水稻高光谱高频组份信号的分离

为了验检高频组份d5在分离不同污染水平的水稻光谱信号的可靠性和普适性，在水稻的分蘖期3个各不相同污染水平的试验区随机选择200条样本光谱数据，每10条求平均，而后对3个污染水平的各20组数据在波长350—1300 nm范围内进行“Db5”函数第5层小波分解，得到d5光谱曲线，图4是原始光谱和d5光谱曲线。由图4(a)可见，3种不同铅污染水平的原始反射率在350—1300 nm波段范围交织在一起未发生显著地分离现象，尤其是中污染水平的水稻光谱反射率交错分布在高和低污染水平的水稻光谱反射率中。而原始光谱信号经小波变换后的高频组份d5有效地分离了不同铅污染水平的水稻光谱信号(图4(b))，尤其在680 nm、700 nm、730 nm、1120 nm、1150 nm和1180 nm附近发生显著的差异。由图4(b)进一步可知，对于相同污染水平的d5曲线形成了紧密的一簇，显而易见高频部分d5表现出来的特征是3簇相对独立的曲线，这主要是由于同一重金属污染等级对作物影响的一致性与不同重金属污染等级对作物影响的差异性所致。

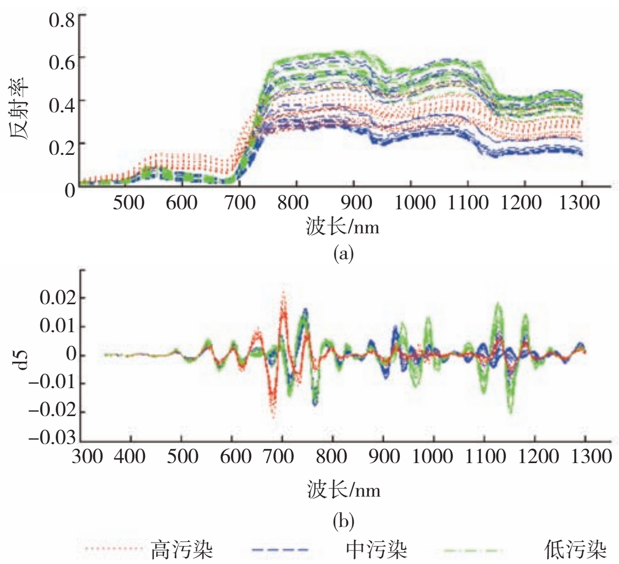

图4 不同污染水平的水稻反射率曲线和d5曲线

(a) 原始反射率曲线；(b) d5曲线

3.4 不同铅污染胁迫水平水稻高光谱高频组份的分维数分析

为了验证试验的稳定性和可靠性，分别采集了实验区2008年和2009年的水稻在出苗期、分蘖期、拔节期、开花期和成熟期等各生长期的高光谱数据，对高光谱测试数据求其平均后再进行小波变换和分维数的计算。根据前面分析和已有的研究，分蘖期是探测水稻重金属胁迫的最佳时期(刘美玲 等，2010)，因而本文仅对水稻两年中的分蘖期d5曲线进行分维数统计和分析(图5)。从图5可见，2008年和2009年高、中和低三个污染水平的分维数都有明显的差异，而同一污染水平的分维数分布相对集中，这是由于d5曲线在3个不同重金属污染水平下形成的3簇紧密而相对独立的曲线。为了详细地探讨分维数在不同生长年份对作物重金属污染胁迫反应的稳定性，在此采用同一污染水平的不同年份的年际变化率来度量其稳定性，分维数年际变化率越小，稳定性越好。年际变化率的计算公式如下：

$$\alpha = D_{09} - D_{08} \tag{3}$$

$$\alpha' = \frac{|D_{09} - D_{08}|}{D_{08}} \times 100\% \tag{4}$$

式中，α、α'分别表示分维数的绝对变化和相对变化率，D_{08}和D_{09}分别表示2008年和2009年的分维数。根据式(3)和(4)对图5进行详细统计(表4)。由表4可见，在2008年和2009年，分维数的平均值均是高污染<中污染<低污染，2009年相对于2008年的分维数的年际变化较少，从绝对变化情况看，高和低污染水平的分维数略有减少，而中污染水平的分维数略有增加；从相对变化率情况看，3个污染水平的分维数相对变化率均低于4%，说明高谱组份d5的分维数可以作为检测重金属胁迫水平的一个稳定参数，能有效地剥离不同年份气象条件的差异。在3个污染水平中，中污染水平的分维数年际相对变化率略大于高污染和低污染水平，可能原因是，铅对水稻的影响表现在“低促高

抑”，低浓度和高浓度的铅胁迫对水稻造成的影响相对较稳定，而中浓度铅胁迫的水稻在色素、细胞结构和植株结构等生理功能处于逐渐被胁迫的阶段，而胁迫的程度会受外界环境因素的影响(如气温、光照和水分等)。

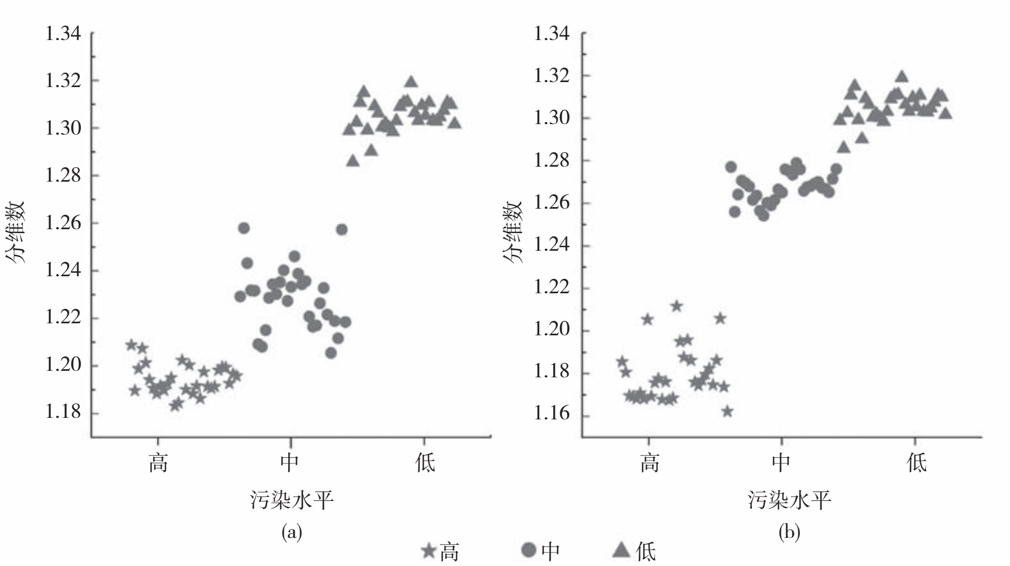

图5 不同污染水平的水稻光谱d5分维数散点图

(a) 2008年；(b) 2009年

表4 不同污染水平的水稻光谱d5分维数统计

年份	统计量	高污染	中污染	低污染
2008	范围	1.183—1.209	1.206—1.258	1.286—1.319
	平均值	1.194	1.229	1.305
	标准差	0.006	0.013	0.006
2009	范围	1.162—1.212	1.254—1.279	1.277—1.309
	平均值	1.179	1.267	1.293
	标准差	0.013	0.006	0.010
年际变化*	绝对变化	–0.015	0.038	–0.012
	相对变化率/%	1.26	3.09	0.92

*表示2009年相对于2008年分维数的变化。

3.5 光谱高频组份的分维数与水稻污染胁迫水平的关系

为了建立高频组份d5的分维数与水稻污染胁迫水平之间的相互关系，以2008年水稻高光谱样本数据(n=90)为基础，利用升(降)半阶隶属度函数建立d5的分维数与水稻污染胁迫水平的数学模型。

分维数对水稻遭受铅污染高度胁迫水平的隶属度函数：

$$u(D_i)=\begin{cases}1 & D_i\leqslant 1.200\\ \dfrac{1.220-D_i}{1.220-1.200} & 1.200<D_i<1.220\\ 0 & D_i>1.220\end{cases}\tag{5}$$

分维数对水稻遭受铅污染中度胁迫水平的隶属度函数：

$$u(D_i)=\begin{cases}\dfrac{D_i-1.200}{1.220-1.200} & 1.200<D_i<1.220\\ 1 & 1.220\leqslant D_i\leqslant 1.275\\ \dfrac{1.280-D_i}{1.280-1.275} & 1.275<D_i<1.280\\ 0 & D_i<1.200,\ D_i>1.280\end{cases}\tag{6}$$

分维数对水稻遭受铅污染低度胁迫水平的隶属度函数：

$$u(D_i)=\begin{cases}0 & D_i\leqslant 1.275\\ \dfrac{D_i-1.275}{1.280-1.275} & 1.275<D_i<1.280\\ 1 & D_i\geqslant 1.280\end{cases}\tag{7}$$

为验证上述模型在不同生长年份条件下的可靠性和适用性，采用2009年不同生长期的观测数据对模型进行检验。对3个污染水平的模糊数学预测水平的判别精度进行了统计(表5)，从表5可知，高、中和低3个污染水平模糊数学预测水平的判别精度依此为93.33%、93.33%和96.67%。通过隶属度函数建立水稻铅污染胁迫水平数学模型具有较高的判别精度，能够达到监测水稻铅污染胁迫状况的目的。

为了更加准确地衡量高光谱分维数与胁迫水平之间的关系，对2008和2009年两年的3个污染胁迫水平的水稻光谱d5的分维数进行频率分布统计(图6)。从图6(a)—(c)中可知,高、中和低污染水平的d5分维数分别主要集中在1.160—1.200、1.220—1.275和1.280—1.320之间，它们的频率各占86.7%、75%和91.7%；从3个污染水平的d5分维数整体情况看，d5分维数的差异在中间过渡中存在不分明性，高与中、中与低之间存在着交叉现象(图6(d))，交叉区域分别是1.200—1.220和1.275—1.280。对于这类污染胁迫水平分级界线不明确的问题，用模糊数学的方法，采用隶属度函数来描述水稻重金属污染胁迫水平，体现了其实际界限的模糊性，具有综合、客观的特点，使评价结果合理、可信，更符合实际需要。

表5 不同污染胁迫水平隶属度函数模糊模型验检

实验样区	样本数	实际污染水平	模糊数学预测污染水平		判别精度
			预测水平	样本数	
A	30	高	高	28	93.33%
			中	2	
			低	0	
B	30	中	高	0	93.33%
			中	28	
			低	2	
C	30	低	高	0	96.67%
			中	1	
			低	29	

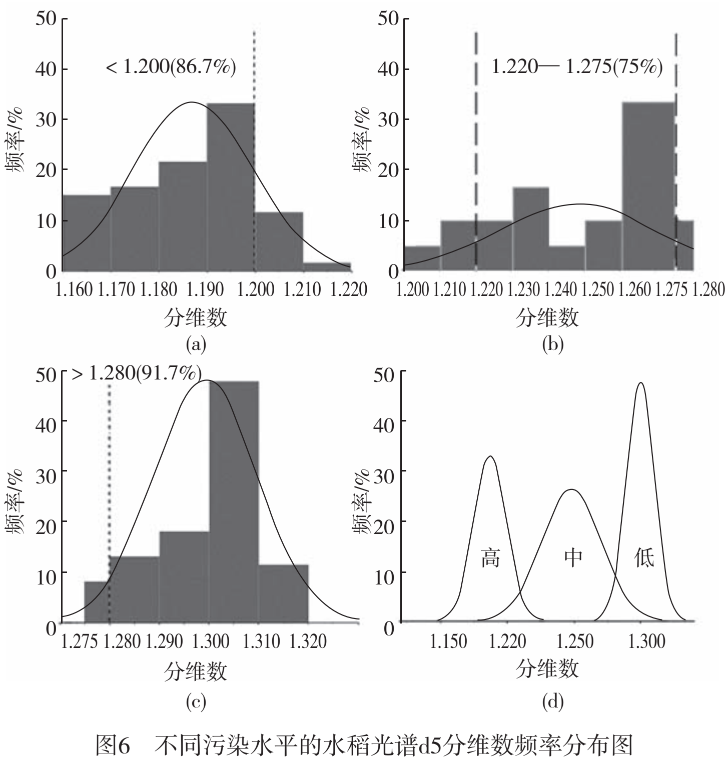

图6 不同污染水平的水稻光谱d5分维数频率分布图

（a）高污染；（b）中污染；（c）低污染；（d）三种污染水平

4 结 论

(1)水稻高光谱反射率的第5层高频组份d5能够剔除其他环境因素(如光照、温度、水分等气象条件)对光谱产生的影响，有效提取水稻重金属胁迫光谱弱信息，进而实现不同污染水平的高光谱信息分离，表明了小波变换技术在高光遥感去噪和提取弱信息中有着广泛的应用前景。相对于传统导数变换消噪的方法、直接利用原始光谱反射率或植被指数的方法(刘素红 等，2007；李庆亭 等，2008；Chi 等，2009)，小波变换

技术对作物重金属污染胁迫水平的诊断研究有明显优势：第一，小波变换提取的作物光谱高谱组份适合探测“自然农田生态系统”中浓度相对较低的重金属污染水平，不再局限于识别高污染胁迫水平的作物，而且该方法可推广到各种环境胁迫下所引起的作物异常探测和弱信息增强。第二，小波变换能对提取的作物光谱异常现象出现的特定波段进行准确的定位，有利于开展不同重金属污染源所导致的光谱差异研究。

(2)高光谱数据d5的分维数能定量地反应水稻在同一生长年份各个生长期遭受重金属污染胁迫的光谱细微差异。同时在2008年和2009年两年中，高光谱数据d5的分维数对于同一污染水平的年际相对变化率小于4%，对于不同污染水平的区分度大于75%，即在高、中和低污染水平中86.7%、75%和91.7%分布在1.160—1.200、1.220—1.275和1.280—1.320三个区间。这表明d5的分维数是一个既稳定又敏感的光谱参数，原因主要有以下两个方面：第一，小波变换获得的高频组份有极强的局部细化能力，放大了重金属污染胁迫弱信息；第二，d5曲线中的350—1300 nm的分维数反映了光谱信号奇异性的整体变化，它有别于单个波段或植被指数摒弃了光谱的大部分有用信息瑕疵(Kemper和Sommer，2002；Slonecker 等，2009)。

(3)采用升(降)半梯形分布的隶属度函数建立了d5分维数与高、中和低3个污染胁迫水平的数学模型，便于解决1.200—1.220和1.275—1.280两个重叠区域的分维数与污染胁迫水平的相关关系。且经过模型精度检验，其判别精度大于90%。采用隶属度来描述不同胁迫水平差异的过渡状态,符合作物胁迫水平中各因素间的不确定性、随机性和模糊性,可以作为处理作物环境胁迫水平评价中模糊性问题的有力手段。

综上所述，利用小波变换、分形分析和模糊数学三者相结合有效地实现了光谱弱信息提取、度量及建模，达到水稻重金属污染胁迫状况监测的目的。本文提出的利用高光谱高频组份分维数建立的隶属度函数评价重金属污染胁迫水平的模型外推到其他地区时，需要依据不同的作物类型和不同的污染源进行修订。该模型不仅可以直接应用于近地面观测的高光谱遥感实测数据分析，还可应用到经过大气校正等参数订正后的星载或机载高光谱遥感影像数据分析。

REFERENCES

Borodich F M. 1997. Some fractal models of fracture. *Journal of the Mechanics and Physics of Solids*, **45**(2): 239–259

Chen S N, Liu X H, Hou J, Liu X H, Chi G Y, Cui B S and Yang Z F. 2007. Study on the spectrum response of *Brassica Campestris* L. leaf to the zinc pollution. *Spectroscopy and Spectral Analysis*, **27**(9): 1797–1801

Chi G Y, Chen X, Shi Y and Liu X H. 2009. Spectral response of rice (*Oryza sativa* L.) leaves to Fe^{2+} stress. *Science in China Series C-Life Sciences*, **52**(8): 747–753

Choe E, van der Meer F, van Ruitenbeek F, van der Werff H, de Smeth B and Kim Y W. 2008. Mapping of heavy metal pollution in stream sediments using combined geochemistry, field spectroscopy, and hyperspectral remote sensing: a case study of the Rodalquilar mining area, SE Spain. *Remote Sensing of Environment*, **112**(7): 3222–3233

Clevers J G P W, Kooistra L and Salas E A L. 2004. Study of heavy metal contamination in river floodplains using the red–edge position in spectroscopic data. *International Journal of Remote Sensing*, **25**(19): 3883–3895

Collins W, Chang S H, Raines G L, Canney F and Ashley R. 1983. Airborne biogeophysical mapping of hidden mineral deposits. *Economic Geology*, **78**(4): 737–749

Daubechies I. 1990. The wavelet transform, time-frequency localization and signal analysis. *IEEE Transactions on Information Theory*, **36**(5): 961–1005

Du H Q, Jin W, Ge H L, Fan W Y and Xu X J. 2009. Using fractal dimensions of hyperspectral curves to analyze the healthy status of vegetation. *Spectroscopy and Spectral Analysis*, **29**(8): 2136–2140

Dunagan S C, Gilmore M S and Varekamp J C. 2007. Effects of mercury on visible/ near-Infrared reflectance spectra of mustard spinach plants (*Brassica rapa* P.). *Environmental Pollution*, **148**(1): 301–311

Guan L and Liu X N. 2009. Experimental research on remote sensing diagnosis method of Cd pollution stress in rice. *Transactions of the Chinese Society of Agricultural Engineering*, **25**(6): 168–173

Kemper T and Sommer S. 2002. Estimate of heavy metal contamination in soils after a mining accident using reflectance spectroscopy. *Environmental Science and Technology*, **36**(12): 2742–2747

Kooistra L, Salas E A L, Clevers J G P W, Wehrens R, Leuven R S E W. Nienhuis P H and Buydens L M C. 2004. Exploring field vegetation reflectance as an indicator of soil con tamination in river floodplains. *Environmental Pollution*, **127**(2): 281–290

Kooistra L, Wehrens R, Leuven R S E W and Buydens L M C. 2001. Possibilities of visible-near-infrared spectroscopy for the assessment of soil contamination in river floodplains. *Analytica Chimica Acta*, **446**(1–2): 97–105

Li Q T, Yang F J, Zhang B , Zhang X and Zhou G Z. 2008. Biogeochemistry responses and spectral characteristics of Rhus Chinensis Mill under heavy metal. *Journal of remote sensing*, **12**(2): 284–290

Liu M L, Liu X N, Li T and Xiu L N. 2010. Analysis of hyperspectral singularity of rice under Zn pollution stress. *Transactions of the Chinese Society of Agricultural Engineering*. **26**(3): 191–197

Liu S H, Liu X H, Hou J, Chi G Y and Cui B S. 2007. Study on the spectral response of *Brassica Campestris* L. leaf to the copper pollution. *Science in China Series E: Technological Sciences*, **37**(5): 693–699

Montzka C, Canty M, Kreins P, Kreins P, Kunkel R, Menz G, Vereecken H and Wendland F. 2008. Multispectral remotely sensed data in modelling the annual variability of nitrate concentrations in the leachate. *Environment modeling and software*, **23**(8): 1070–1081

Noh H, Zhang Q, Shin B, Han S and Feng L. 2006. A neural network model of maize crop nitrogen stress assessment for a multi-spectral imaging sensor. *Biosystems Engineering*, **94**(4): 477–485

Osborne S L, Schepers J S, Francis D D and Schlemmerb M R. 2002. Detection of phosphorus and nitrogen deficiencies in corn using spectral radiance measurements. *Agronomy Journal*, **94**(6): 1215–1221

Qi Y B, Huang B, Darilek J L and Wang Z G. 2008. Comparison of heavy metal fractions distribution in paddy soil under anoxic and oxidized conditions. *Ecology and Environment*, **17**(6): 2228–2233

Ren H Y, Zhuang D F, Pan J J, Shi X Z and Wang H J. 2008. Hyperspectral remote sensing to monitor vegetation stress. *Journal of Soils and Sediments*, **8**(5): 323–326

Schuerger A C , Capelle G A , Di Benedetto J A , Mao C Y, Thai C N, Evans M D, Richards J T, Blank T A and Stryjewski E C. 2003. Comparison of two hyper-spectral imaging and two laser-induced fluorescence instruments for the detection of zinc stress and chlorophyll concentration in bahia grass (*Paspalum notatum* Flugge.). *Remote Sensing of Environment*, **84**(4): 572–588

Slonecker T, Haack B and Price S. 2009. Spectroscopic analysis of arsenic uptake in pteris ferns. Remote Sensing. DOI: 10.3390/rs1040644

van der Meer F. 2006. Indicator kriging applied to absorption band analysis in hyperspectral imagery: a case study from the Rodalquilar epithermal gold mining area, SE Spain. *International Journal of Applied Earth Observation and Geoinformation*, **8**(1): 61–72

Wang L, Lin Q Z, Jia D, Shi H S and Huang X H. 2007. Study on the prediction of soil heavy metal elements content based on reflectance spectra. *Journal of remote sensing*, **11**(6): 906–913

Wang M Q and Zhang M K. 2002. Concentrations and chemical associations of heavy metals in urban and suburban soils of the Hangzhou City, Zhejiang Province. *Acta Scientiae Circumstantiae*, **22**(5): 603– 608

Zhao Q G, Zhou B Z and Yang H. 2002a. Studying on environmental quality and agricultural safety problem in Jiangsu Province. *Soil*, **34**(1): 1–8

Zhao Q G, Zhou B Z, Yang H, Liu S L. 2002b. Some considerations on safety of arable land resources in China: problems and counter-measures. *Soil*, **34**(6): 293–302

附中文参考文献

陈思宁，刘新会，侯娟，刘素红，迟光宇，崔保山，杨志峰. 2007. 重金属锌胁迫的白菜叶片光谱响应研究. 光谱学与光谱分析，**27**(9): 1797–1801

杜华强，金伟，葛宏立，范文义，徐小军. 2009. 用高光谱曲线分形维数分析植被健康状况. 光谱学与光谱分析，**29**(8): 2136–2140

关丽，刘湘南. 2009. 水稻镉污染胁迫遥感诊断方法与试验. 农业工程学报，**25**(6): 168–173

李庆亭，杨锋杰，张兵，张霞，周广柱. 2008. 重金属污染胁迫下盐肤木的生化效应及波谱特征. 遥感学报，**12**(2): 284–290

刘美玲，刘湘南，李婷，修丽娜. 2010. 水稻锌污染胁迫的光谱奇异性分析. 农业工程学报，**26**(3): 191–197

刘素红，刘新会，侯娟，迟光宇，崔保山. 2007. 植物光谱应用于白菜铜胁迫响应研究. 中国科学E辑: 技术科学，**37**(5): 693–699

齐雁冰，黄标，Darilek J L，王志刚. 2008. 氧化与还原条件下水稻土重金属形态特征的对比. 生态环境，**17**(6): 2228–2233

王璐，蔺启忠，贾东，石火生，黄秀华. 2007. 基于反射光谱预测土壤重金属元素含量的研究. 遥感学报，**11**(6): 906–913

王美青，章明奎. 2002. 杭州市城郊土壤重金属含量和形态的研究. 环境科学学报，**22**(5): 603–608

赵其国，周炳中，杨浩. 2002a. 江苏省环境质量与农业安全问题的研究. 土壤，**34**(1): 1–8

赵其国，周炳中，杨浩，刘世亮. 2002b. 中国耕地资源安全问题及相关对策思考. 土壤，**34**(6): 293–302